

FRAMEWORK FOR IMPLEMENTING DAMPING SCALING FACTORS IN U.S. GEOLOGICAL SURVEY NATIONAL SEISMIC HAZARD MODELS

A. J. Makdisi¹, D. N. Smith², S. Rezaeian¹, P. M. Powers¹, & K. B. Withers¹

¹ U.S. Geological Survey, Golden, Colorado, USA, amakdisi@usgs.gov

² Brigham Young University, Provo, Utah, USA

Abstract: Traditionally, probabilistic seismic hazard analysis (PSHA) has focused on calculating ground motion hazard curves for elastic, 5%-damped pseudo spectral accelerations, $S_a(T)_{5\%}$, which are used as the basis for engineering design parameters and targets for ground motion selection and modification. However, structures and geotechnical systems can exhibit a wide range of damping ratios both above and below the 5% level, depending on the construction material, structural system, nonstructural elements, or subsurface soil properties. When spectral parameters at such damping levels are required for certain applications, 5%-damped accelerations have traditionally been extracted from PSHA-based hazard curves and adjusted outside of the hazard integral using damping scaling factors (DSF) such as those from Newmark & Hall (1982). Recent advances in the development of more rigorous and comprehensive damping scaling models (e.g., Rezaeian et al., 2014; Rezaeian et al., 2021) have allowed for the modeling of means and standard deviations of DSFs as functions of earthquake source and path properties for crustal, intraslab, and subduction interface tectonic environments. These DSF models can be applied to ground motion model (GMM) estimates of $S_a(T)_{5\%}$ for a given earthquake rupture scenario to produce a corresponding mean and standard deviation S_a at a specified damping ratio β , $S_a(T)_\beta$. In this study, the DSF models of Rezaeian et al. (2014) and Rezaeian et al. (2021) are implemented within the U.S. Geological Survey National Seismic Hazard Model (NSHM) PSHA framework to calculate probabilistic hazard curves for spectral accelerations at damping ratios from 0.5% to 30%. The DSF models are applied directly to the mean and standard deviation of $S_a(T)_{5\%}$ predictions from each GMM in the NSHM logic tree. Resulting hazard curves and uniform hazard and risk spectra for $S_a(T)_\beta$ are presented for several geographic locations and compared with corresponding spectra estimated using current design practices by applying the same DSFs outside of the PSHA calculation. Key differences between the two methods for estimating $S_a(T)_\beta$ are discussed, and potential strategies are presented for the implementation and usage of the hazard-consistent $S_a(T)_\beta$ in building codes. Comparing the results to those from DSFs used in current design practices that are mainly based on Newmark & Hall (1982) is not explored in this study.

1. Introduction

Seismic design of engineered systems generally requires a simplified representation of the ground motion characteristics that a site of interest might experience in a given tectonic environment. Traditionally these types of analyses require the estimation of ground motion intensity measures (IMs) for a controlling rupture scenario (in deterministic seismic hazard analysis) or for the full set of plausible rupture scenarios (in a probabilistic seismic hazard analysis, or PSHA). Such IM estimates are typically generated via empirical ground motion models (GMMs), the overwhelming majority of which have been developed for elastic pseudo spectral acceleration, at a damping ratio of 5%, $S_a(T)_{5\%}$. $S_a(T)$ represents the peak response of a single-degree-of-freedom oscillator, with the damping ratio β representing the level of energy dissipation in the engineering system of interest (e.g., structure, geotechnical system, or non-structural component). Although a damping ratio of 5% has been considered a reasonable default value for a typical structure in developing design ground motions, the origins of this number are unclear. The reality is that seismic design applications cover a wide

range of systems, including non-building structures such as storage tanks and vessels, non-structural components, and buildings designed using base-isolated systems and damping devices that can have very different damping ratios. These systems exhibit a wide range of dissipation levels, and therefore they may be more appropriately modeled using pseudo spectral accelerations with β values other than 5% (examples provided in Rezaeian *et al.*, 2014). Models of damping scaling factors (*DSF*) have been developed and used to modify the default, 5%-damped, pseudo spectral accelerations to appropriate damping ratios for given engineering systems. In current engineering practice, *DSFs* are applied to design ground motions outside of the PSHA for simplicity, even though they are developed for GMMs that are used inside the PSHA.

This study explores the two different approaches to using *DSF* models: outside of the PSHA as in current engineering practices, and inside the PSHA as the models should be used. Conventional methods for estimating non-5% damped ground motions, wherein design ground motions are modified using *DSF* models outside the PSHA calculation, are presented and their practical considerations and limitations are discussed. A more rigorous method is then proposed, involving direct hazard calculations of non-5% damped ground motions by applying *DSF* models *within* the PSHA calculation, and a preliminary implementation is presented within the U.S. Geological Survey (USGS) National Seismic Hazard Model (NSHM) (e.g., Petersen *et al.*, 2020). Resulting design ground motion spectra using the two methods are compared for several test locations throughout the United States, and potential improvements and impacts to seismic provisions of building codes are discussed. Note that *DSFs* used in current design practices are only period-dependent and are based on outdated models such as the one by Newmark & Hall (1982). These outdated models have been compared with more recent recordings of earthquake ground motions that suggest the models should also depend on magnitude, distance, and tectonic regions (Rezaeian *et al.*, 2014, 2021); however, in this study we do not explore the differences between various *DSF* models and instead focus on the two different applications of the same *DSF* model.

2. Background

While the default damping ratio used in most GMMs and PSHA calculations, and therefore most seismic design applications, is 5%, engineering systems can exhibit a wide range of damping ratios (Rezaeian *et al.*, 2021). Tall, flexible buildings tend to dissipate much less energy when subjected to ground shaking, leading to damping ratios as low as 2.5% (PEER/ATC72-1, 2010), while base-isolated structural systems may exhibit damping ratios much higher than the default 5%. For these examples and other applications (e.g., nuclear facilities, non-structural components), it is often necessary to estimate $S_a(T)$ for damping ratios other than the 5% seen in typical GMMs. This is currently achieved by applying period-dependent *DSFs* to convert $S_a(T)_{5\%}$ to spectral accelerations at various damping ratios, $S_a(T)_\beta$, as follows:

$$DSF(T, \beta\%) = \frac{S_a(T)_\beta}{S_a(T)_{5\%}} \quad (1)$$

Early procedures for scaling 5%-damped spectral accelerations to specified damping ratios (e.g., Newmark & Hall, 1982; Idriss, 1993; Abrahamson & Silva, 1996) formed the basis of damping scaling recommendations in several seismic provisions. These early models provided simplified *DSFs* for a limited range of periods, with no dependence on earthquake rupture parameters. Updated empirical *DSF* models using larger ground motion datasets for shallow crustal (Rezaeian *et al.*, 2014) and subduction zone (Rezaeian *et al.*, 2021) environments (collectively referred to herein as the "NGA" *DSF* models) showed a statistically significant dependence of the *DSF* on earthquake moment magnitude M_w and closest rupture distance R_{rup} , resulting in more rigorous models that incorporate these effects and quantify the variability in estimating *DSF* for a given rupture scenario.

Within the context of design of new structures in the United States, the American Society of Civil Engineers (ASCE) 7 standard (e.g., ASCE, 2022) require development of risk-targeted ground motions for the maximum considered earthquake (MCE_R) response spectrum used as input to structural analyses and design procedures. The MCE_R spectral accelerations are computed by iteratively integrating the probabilistic hazard curves for $S_a(T)_{5\%}$ with a collapse fragility curve that is anchored to a 10% probability of collapse conditioned on the occurrence of the risk-targeted spectral acceleration (Luco *et al.*, 2007). In typical engineering applications, seismic hazard analysis for non-5% damping levels is performed by converting the 5%-damped MCE_R to the damping ratio of interest using an applicable *DSF* model. This "deterministic" approach is defined

here as applying a constant value of DSF to the 5%-damped MCE_R at a given period; such a DSF is either based on older models as described above or precalculated based on a deterministic event. When using a model with additional parameters besides spectral periods, such as the Rezaeian et al. (2014) and Rezaeian et al. (2021) models, this requires disaggregation of hazard to identify the tectonic setting that controls the MCE_R ground motions, which determines the appropriate DSF model to use (i.e., one based on shallow crustal or subduction zone ground motions) and the modal M_w and R_{Rup} . This method is herein referred to as the “hybrid” approach for computing MCE_R spectra at non-5% damping levels, due to the use of probabilistic methods to calculate the initial 5%-damped MCE_R , mixed with deterministic methods to convert it to non-5% damping levels.

MCE_R spectra for a set of damping ratios ranging from 0.5% to 30%, developed using the hybrid procedure described above and the NGA crustal and subduction DSF models, are shown in [Figure 1](#) [Figure 4](#) and [Figure 2](#) [Figure 2](#) for four U.S. cities that feature as test sites for the National Earthquake Hazards Reduction Program (NEHRP) provisions (Building Seismic Safety Council, 2020). Note that for Central and Eastern United States (CEUS) sites such as St. Louis, the NGA active crustal DSF model is used, due to the current lack of a DSF model that applies to stable continental tectonic environments.

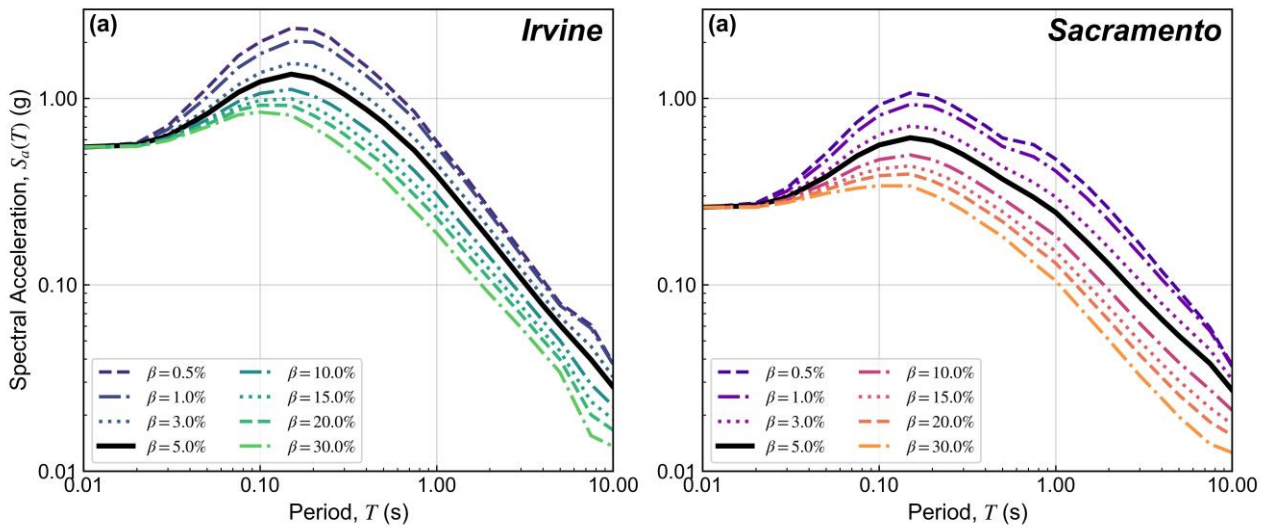


Figure 1: Damped MCE_R spectra for (a) Irvine, California and (b) Sacramento, California NEHRP test cities, developed according to ASCE 7-22 site-specific procedures, with damping scaling factors applied to the 5%-damped MCE_R spectrum using the “hybrid approach”.

While this hybrid procedure for computing the damped MCE_R is necessary given the current state of practice and availability of information in most PSHA computational platforms (e.g., Powers et al., 2022), it is cumbersome for a practicing engineer and requires several assumptions and oversimplifications. Further, the hybrid procedure may produce results inconsistent with more accurate fully probabilistic methods for directly computing $S_a(T)_\beta$ hazard curves by implementing DSF models inside the PSHA directly (refer to Section 3.2). The hybrid simplifications include (1) that a single rupture scenario controls the scaling between 5%- and non-5% damping levels, and (2) that there is no uncertainty in scaling between 5%- and non-5% damping levels. With respect to the first simplification, there is potential for the dominant rupture scenario to vary considerably with oscillator period T and introduce abrupt discontinuities in the DSF -adjusted MCE_R spectrum. This effect is evident in all four of the NEHRP examples shown in [Figure 1](#) [Figure 4](#) and [Figure 2](#) [Figure 2](#) at a variety of periods and damping levels.

A more accurate method for producing uniform-hazard and MCE_R response spectra at specified damping ratios is to instead perform PSHA directly for $S_a(T)_\beta$, accounting for all rupture scenarios, aleatory variabilities, and epistemic uncertainties in the same manner that is commonly performed for the default 5%-damped spectral accelerations. The following sections illustrate how this “probabilistic approach” can be readily achieved using existing PSHA computational infrastructure (e.g., Powers et al., 2022) and DSF models that adjust $S_a(T)_{5\%}$ to $S_a(T)_\beta$ within the hazard integral, directly addressing the limitations in conventional deterministic and hybrid methods for adjusting MCE_R spectra.

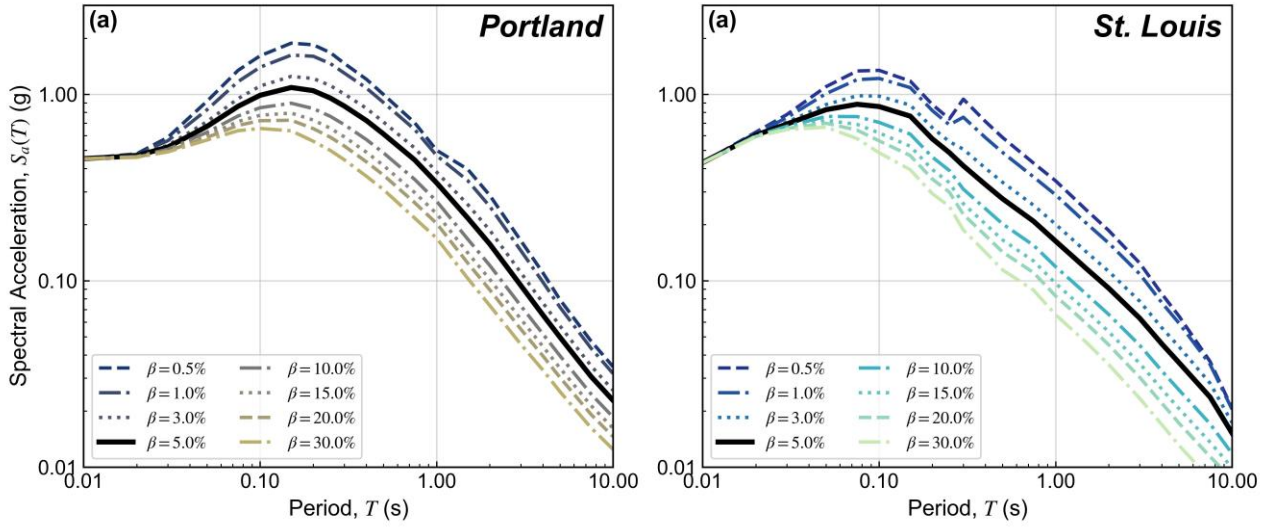


Figure 2: Damped MCE_R spectra for (a) Portland, Oregon, and (b) St. Louis, Missouri, NEHRP test cities, developed according to ASCE 7-22 site-specific procedures, with damping scaling factors applied to the 5%-damped MCE_R spectrum using the “hybrid approach.”

3. Implementation of damping scaling factors in the USGS NSHM

One of the advantages of using the NGA DSF models is that they allow for computation of both median and standard deviation of $S_a(T)_\beta$ for a given rupture scenario, using similar inputs and producing the same type of outputs as what is obtained using many of the GMMs for $S_a(T)_{5\%}$ in current PSHA frameworks. Such DSF models present a convenient and practical method for direct hazard curve computation. Rather than relying on the development of new GMMs that directly estimate $S_a(T)$ for different damping ratios, DSF models can be tied directly to the suites of GMMs that are already validated and used to compute $S_a(T)_{5\%}$ in the USGS NSHM.

3.1. Scenario ground motion predictions using damping scaling factors

The functional form of the empirical NGA DSF models can be expressed as follows:

$$\ln DSF(T, \beta) = \mu(T, \beta\%, M_w, R_{Rup}, b) + \varepsilon \cdot \sigma_{\ln DSF} \quad (2)$$

where M_w and R_{Rup} are the moment magnitude and closest rupture distance, respectively, of the given rupture scenario; b is the set of model coefficients, which depend on the tectonic environment with different coefficients for shallow crustal (Rezaeian et al., 2014) and subduction interface or intraslab (Rezaeian et al., 2021) ground motions; ε is a standard normal distribution assumed to have zero mean and a standard deviation of 1; and $\sigma_{\ln DSF}$ is the DSF model standard deviation. The median DSF , μ , is also period-dependent and can be computed for a range of damping ratios, from $\beta=0.5\%$ to 30%. The resulting median and logarithmic standard deviation values of the damped spectral acceleration $S_a(T)_\beta$, denoted as $\mu_{\ln S_a(T)_\beta}$ and $\sigma_{\ln S_a(T)_\beta}$, respectively, are computed by combining the median and logarithmic standard deviation of the DSF model with those of the GMM-based estimate of $S_a(T)_{5\%}$ for the same rupture scenario and vibration period (T), as follows:

$$\mu_{\ln S_a(T)_\beta} = \mu_{\ln S_a(T)_{5\%}} + \mu_{\ln DSF(T)} \quad (3a)$$

$$\sigma_{\ln S_a(T)_\beta} = \sqrt{\sigma_{\ln S_a(T)_{5\%}}^2 + \sigma_{\ln DSF}^2 + 2\sigma_{\ln S_a(T)_{5\%}}\sigma_{\ln DSF}\rho} \quad (3b)$$

where $\mu_{\ln S_a(T)_{5\%}}$ and $\sigma_{\ln S_a(T)_{5\%}}$ are the median and log standard deviation GMM-based estimates of 5%-damped spectral acceleration; and ρ is the correlation coefficient between $\ln DSF$ and $\ln S_a(T)_{5\%}$, which is provided as tabular data in Rezaeian et al. (2014) and Rezaeian et al. (2021). Example mean and plus/minus one standard deviation response spectrum predictions are shown in [Figure 3](#) for crustal and subduction earthquake scenarios. The response spectra predictions for the crustal scenario ([Figure 3a](#)) are computed using a subset of the Next Generation Attenuation West (NGA-West2) GMMs (Abrahamson

et al., 2014; Boore et al., 2014; Campbell & Bozorgnia, 2014; Chiou & Youngs, 2014) and the Rezaeian et al. (2014) *DSF* model. The corresponding subduction-zone scenario predictions in [Figure 3](#) were computed using Next Generation Attenuation Subduction (NGA-Sub) GMMs (Abrahamson & Gulerce, 2022; Kuehn et al., 2023; Parker et al., 2022) and the Rezaeian et al. (2021) *DSF* model. For illustration purposes only, in the figure the median spectra are computed from the mean of the individual GMM $\ln S_a(T)_\beta$ values, while the standard deviation is computed as the mean of the individual GMM values of $\sigma_{\ln S_a(T)_\beta}$.

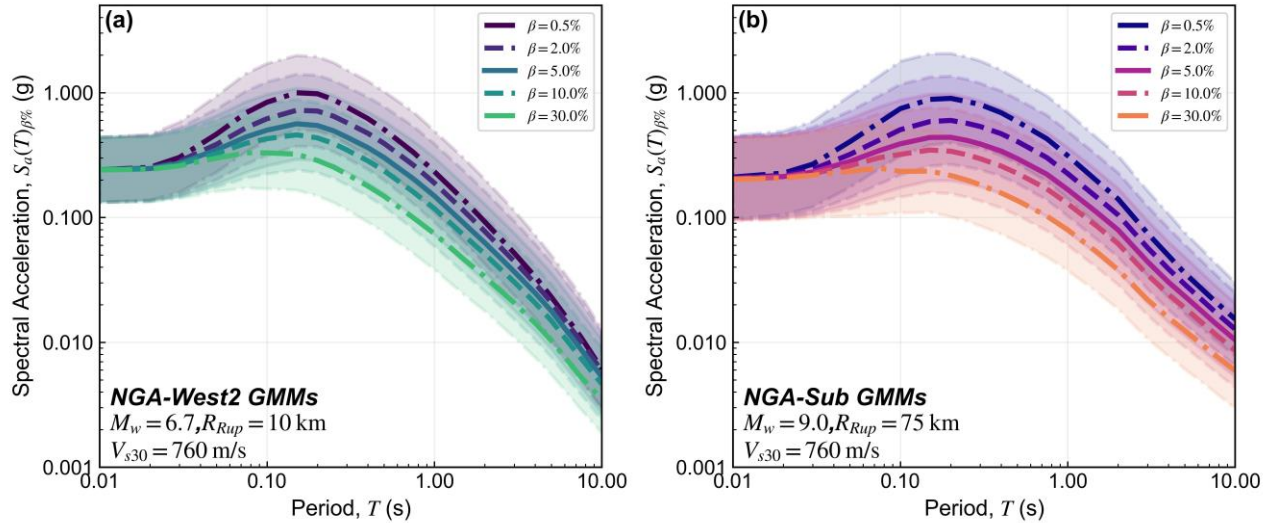


Figure 3: Weighted average median and standard deviation response spectra for a range of damping ratios for a hypothetical site with an average shear wave velocity in the upper 30 m (V_{s30}) of 760 m/s and scenarios corresponding to (a) a shallow crustal earthquake, combining NGA-West2 GMMs with the Rezaeian et al. (2014) *DSF* model, and (b) a subduction interface earthquake, combining NGA-Subduction (NGA-Sub) GMMs with the Rezaeian et al. (2021) *DSF* model. Shaded regions represent \pm one standard deviation.

3.2. Implementation of *DSF* GMMs in the USGS NSHM

The combination of the NGA *DSF* models with existing NGA-West2 and NGA-Sub GMMs (refer to [Figure 3](#)) results in suites of ground motion predictions of $S_a(T)$ at specified damping ratios that capture an important source of epistemic uncertainty in the median and standard deviation estimates of $S_a(T)_\beta$. In this manner, logic trees for conventional 5%-damped GMMs can essentially be replicated by scaling the $S_a(T)_{5\%}$ predictions to $S_a(T)_\beta$ using Equations (2) and (3a) for each GMM in the logic tree for all rupture scenarios. However, additional potential sources of epistemic uncertainty that may stem from other models for computing non-5% damped ground motions are neglected here. Example logic trees for the damped $S_a(T)$ computations are shown for shallow crustal and subduction zone sources in [Figure 4](#). This procedure allows standard PSHA calculations to be performed for $S_a(T)_\beta$ in a similar fashion to current calculation procedures for $S_a(T)_{5\%}$, producing the same types of output (i.e., hazard curves and disaggregation data) that engineers and researchers typically need for $S_a(T)_{5\%}$ and other conventional IMs.

In this study, the NGA *DSF* models were implemented in the USGS NSHM computational platform, `nshmp-haz` (Powers et al., 2022). Median and standard deviation estimates of $S_a(T)_\beta$ were calculated by applying the Rezaeian et al. (2014) *DSF* model to the GMM logic trees for both active crustal sources in the western United States (WUS) and stable continental source in the CEUS, and the Rezaeian et al. (2021) *DSF* model to subduction zone sources in the WUS.

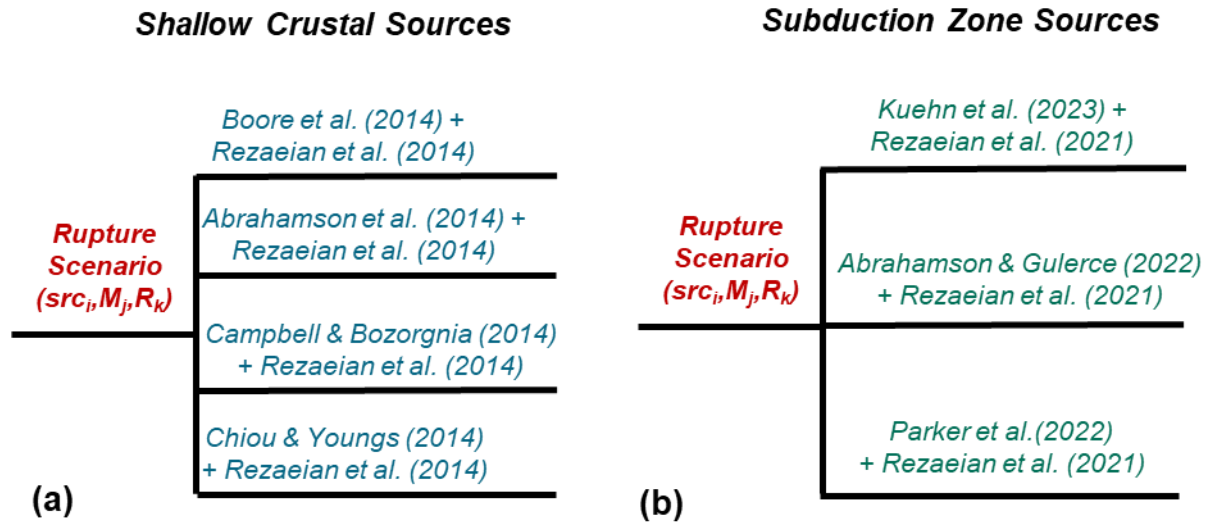


Figure 4: Example logic tree implementation for combining GMM estimates of 5%-damped spectral acceleration with NGA damping scaling models to generate ground motion predictions of spectral acceleration at specified damping ratios for (a) shallow crustal sources (using NGA-West2 GMMs) and (b) subduction zone sources (using NGA-Sub GMMs).

3.3. Hazard calculations for non-5%-damped spectral acceleration in the USGS NSHM

Using the basic GMM implementation framework outlined in Sections 3.1 and 3.2, hazard curves for $S_a(T)_\beta$ were computed in `nshmp-haz` for the same four NEHRP test cities shown in [Figure 1](#) [Figure-4](#) and [Figure 2](#) [Figure-2](#), using the 2018 edition of the NSHM (Petersen et al., 2020) and the associated conterminous United States (CONUS) source catalogue (Powers & Altekruze, 2022). The hazard curve computation for a given IM involves calculating the annualized rate of exceedance λ_{IM} of a range of IM levels for all plausible rupture scenarios rup over all seismic sources src , which can be expressed via:

$$\lambda_{IM}(im) = \sum_i^{N_{src}} \sum_j^{N_{rup}} P[IM > im | rup_{i,j}] \lambda(rup_{i,j}) \tag{4}$$

where the first term within the summation ($P[IM > im | rup_{i,j}]$) is computed for $S_a(T)_\beta$ using the median and log standard deviation predictions in Equation [\(3a\)](#) [\(3\)](#), or alternatively a GMM that directly estimates the median and log standard deviation of $S_a(T)_\beta$. The resulting damped hazard curves for spectral accelerations at two common oscillator periods (0.2 and 1.0 s) are shown for the Irvine, California and Portland, Oregon test sites in [Figure 5](#) [Figure-5](#) and [Figure 6](#) [Figure-6](#), respectively. The hazard curves exhibit the same trends with respect to damping ratio that are implied by the NGA *DSF* models (refer to [Figure 3](#) [Figure-3](#)), with higher annualized rates of exceedance of $S_a(T)_\beta$ at lower damping ratios; conversely, for a given rate of exceedance, the uniform hazard values of $S_a(T)_\beta$ decrease with increasing levels of damping and energy dissipation (i.e., increasing β).

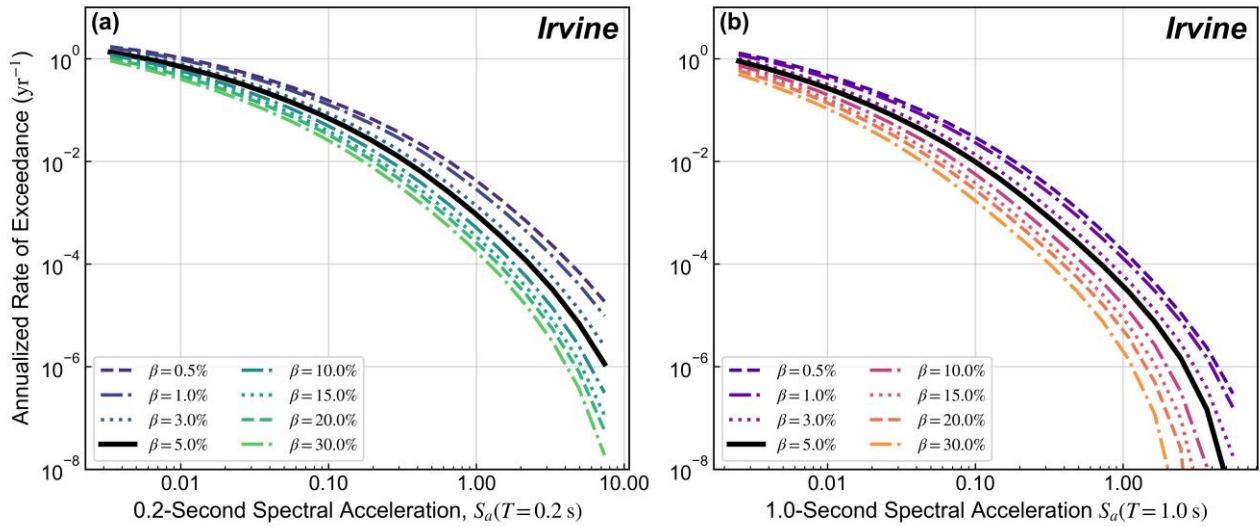


Figure 5: Hazard curves for (a) $S_a(0.2s)$ and (b) $S_a(1.0s)$ at a range of damping ratios, computed using the 2018 USGS NSHM and NGA damping scaling models, for the Irvine, California NEHRP test location.

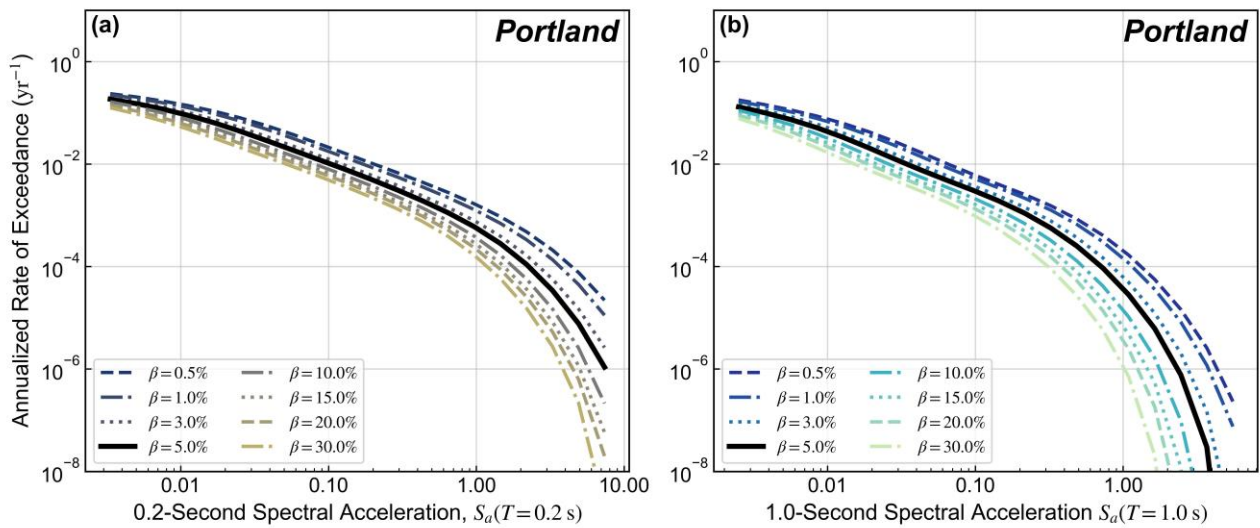


Figure 6: Hazard curves for (a) $S_a(0.2s)$ and (b) $S_a(1.0s)$ at a range of damping ratios, computed using the 2018 USGS National Seismic Hazard Model and NGA damping scaling models for the Portland, Oregon, NEHRP test location.

Comparison between current and proposed procedures for computing damped MCE_R spectra

Using the PSHA calculation results for the non-5% damped spectral acceleration, a fully probabilistic MCE_R spectrum for $S_a(T)_\beta$ can be computed using the iterative integration procedure described in Section 2 (Luco et al., 2007). In [Figure 7](#) and [Figure 8](#) for the four NEHRP test cities, these spectra are compared to the current hybrid methods outlined in Section 2, in which the MCE_R spectrum for $S_a(T)_{5\%}$ is converted to specified damping ratios using the *DSF* models and disaggregation data. Generally, the fully probabilistic approach results in wider ranges of MCE_R ground motions with respect to damping ratio. This indicates that the current hybrid approach underrepresents the sensitivity of the MCE_R ground motions to damping ratio at certain sites and certain period ranges. The underrepresentation is in part because the uncertainty in the *DSF* models is neglected, along with consideration of the full distribution of M_w and R in all rupture scenarios in the hazard integral. Furthermore, because the proposed probabilistic approach scales $S_a(T)_{5\%}$ to $S_a(T)_\beta$ for all sources and rupture scenarios *within* the hazard integral, and there is no need to select a single controlling

rupture scenario to convert the 5%-damped MCE_R , the resulting damped spectra are much smoother, avoiding any of the discontinuities that the hybrid-based MCE_R spectra exhibit at certain sites and period ranges.

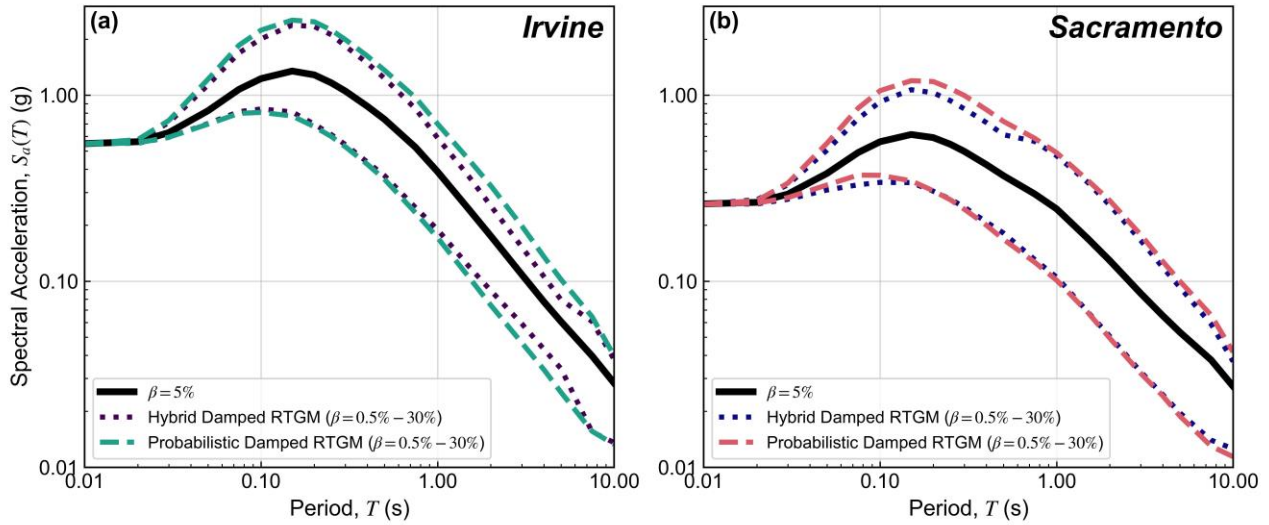


Figure 7: Comparisons of damped MCE_R spectra for (a) Irvine, California, and (b) Sacramento, California, NEHRP test cities, developed using the current “hybrid” approach and the “probabilistic” approach proposed herein. The dashed lines correspond to the 0.5% and 30% damped MCE_R ground motions range.

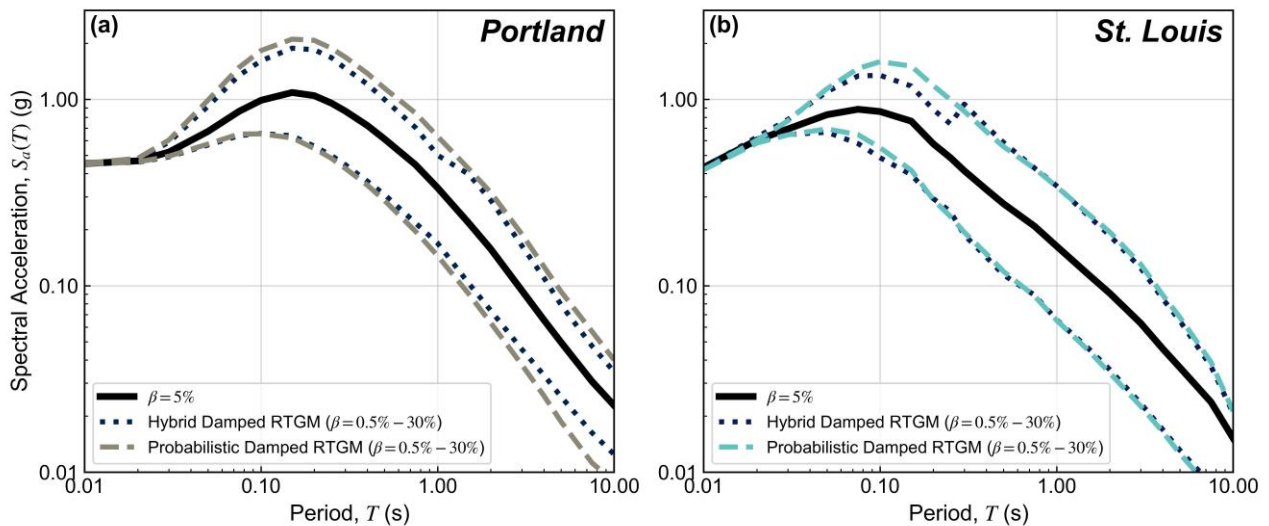


Figure 8: Comparisons of damped MCE_R spectra for (a) Portland, Oregon, and (b) St. Louis, Missouri, NEHRP test cities, developed using the current “hybrid” approach and the “probabilistic” approach proposed herein. The dashed lines correspond to the 0.5% and 30% damped MCE_R ground motions range.

4. Summary, discussion, and concluding remarks

This study presents a preliminary implementation framework within the USGS NSHM for performing full PSHA hazard curve calculations for spectral accelerations at specified damping ratios, $S_a(T)_\beta$. The motivation for this new implementation stems from the somewhat simplistic methods used in current practice for adjusting the 5%-damped uniform hazard or MCE_R ground motion spectra that are typically available from the NSHM and many other PSHA implementations. These methods, described in this study as “hybrid” methods, either (i) use legacy damping scaling models, developed from relatively limited ground motions datasets that do not account for source and path effects, or (ii) employ more recent models that do account for such effects, but require

engineers to make decisions about what “controlling scenario” to select in order to use the damping models outside of the PSHA hazard integral.

The hazard calculations for $S_a(T)_\beta$ were implemented in the USGS `nshmp-haz` software and demonstrated using the 2018 NSHM edition. The implementation follows a conditional GMM framework, where GMMs include conventional $S_a(T)_{5\%}$ values as predictive parameters (e.g., Liu & Macedo, 2021). This allows for the use of existing epistemic uncertainties that are available in conventional $S_a(T)_{5\%}$ predictions using existing GMMs to, at least partially, capture epistemic uncertainties in the prediction of more novel *IMs*. In the case of $S_a(T)_\beta$, this implementation involved combining the NGA *DSF* models of Rezaeian et al. (2014) and Rezaeian et al. (2021) with existing suites of GMMs for 5%-damped spectral accelerations (i.e., NGA-West2, NGA-Sub, NGA-East), resulting in median and lognormal standard deviation estimates of $S_a(T)_\beta$ for all rupture scenarios, all sources, and all GMMs within the hazard curve calculation integral. The resulting damped hazard curves were then iteratively integrated with the notional collapse fragility curves to obtain the non-5% damped MCE_R spectra for a range of damping ratios; this overall approach for developing the MCE_R for specified damping ratios has been described in this study as the “probabilistic” method.

Comparison of the MCE_R ground motion spectra developed using the current hybrid and proposed probabilistic methods for several NEHRP test cities showed that the hybrid method tends to underrepresent the sensitivities to β in computing MCE_R spectra for $S_a(T)_\beta$ relative to the more accurate probabilistic method. Furthermore, the probabilistic method produces smoother MCE_R spectra that are not dependent on how the “controlling” scenario is characterized for selection of appropriate *DSF* parameters. Overall, the preliminary implementation demonstrates that hazard calculations for $S_a(T)_\beta$ can be carried out in a very similar manner as the conventional $S_a(T)_{5\%}$ calculations, producing the same types of output data (e.g., hazard curves, disaggregation).

4.1. Implications for engineering design and seismic provisions

A finalized implementation of hazard curve and disaggregation calculations of $S_a(T)_\beta$ for the USGS NSHM has the potential to substantially improve the current seismic provisions for handling structures and systems with damping ratios other than 5%. While it is recognized that spectral accelerations at damping ratios closer to that of the system of interest are more appropriate for the analysis and design of those systems than the default 5% damping level, the reliance on simplified adjustment factors outside of the PSHA calculation does not guarantee hazard- or performance-consistent ground motions for such systems. Direct computation of probabilistic damped spectral accelerations would address this particular limitation; this improvement can be considered analogous to the improvements made to address the limitations in deterministic site amplification factors (Tables 11.4.-1 and 11.4-2) as recently as ASCE 7-16 (ASCE, 2016), which resulted in fully probabilistic ground motions computed for each site class starting in ASCE 7-22 (ASCE, 2022).

The availability of probabilistic MCE_R ground motions at a range of damping levels may enable improvements to several areas of the current NEHRP provisions and ASCE 7 standard, including non-building structures (Chapter 15), non-structural components (Chapter 13), base-isolated structures (Chapter 17), and structures with damping systems (Chapter 18). The proposed improvements for $S_a(T)_\beta$ also may facilitate more consistency in using spectra at non-5% levels as targets for ground motion selection, through more direct computation of conditional mean and scenario spectra using the same methods that currently exist for computing 5%-damped conditional spectra.

4.2. Future directions

While the results of this preliminary implementation show clear differences on visual inspection when non-5% damped MCE_R ground motions are developed using the hybrid and probabilistic methods for the four NEHRP test sites considered, more systematic evaluation of the differences is needed before developing specific recommendations to the building code development community. Future refinements to this procedure should focus on finalizing and documenting the implementation of $S_a(T)_\beta$ calculations in the 2023 update of the USGS NSHM, and comprehensively quantifying the differences between hybrid and probabilistic procedures for the full set of NEHRP test cities and site classes. Furthermore, the comparisons made in this study focused solely on the application of the NGA *DSF* models; future evaluations of the two procedures should account for the fact that a wider range of damping scaling models and methods are used (e.g., Abrahamson & Silva, 1996; Idriss, 1993), with different simplifications of these methods for recommended use in different design guidelines. The development and evaluation of the probabilistic $S_a(T)_\beta$ procedure should also consider use

cases outside of the NEHRP provisions, and similarly quantify the differences between hybrid and probabilistic procedures through the lens of design spectra computed according to other bases of design, such as ASCE 41 (ASCE, 2017) and the American Association of State Highway and Transportation Officials specifications (AASHTO, 2023).

5. Acknowledgments

The authors would like to acknowledge and thank N. Simon Kwong, Allison Shumway, Nicolas Luco, Brian Shiro, and Janet Carter for their thoughtful comments and feedback, which greatly improved this paper. Any use of trade, firm, or product names is for descriptive purposes only and does not imply endorsement by the U.S. Government.

6. References

- Abrahamson, N. A., & Gulerce, Z. (2022). Summary of the Abrahamson and Gulerce NGA-SUB ground-motion model for subduction earthquakes. *Earthquake Spectra*, 38(4), 2638–2681. <https://doi.org/10.1177/87552930221114374>
- Abrahamson, N. A., & Silva, W. J. (1996). *Section 4: Spectral scaling for other damping values, 455 in Empirical Ground Motion Models*. Brookhaven National Laboratory.
- Abrahamson, N. A., Silva, W. J., & Kamai, R. (2014). Summary of the ASK14 Ground Motion Relation for Active Crustal Regions. *Earthquake Spectra*, 30(3), 1025–1055. <https://doi.org/10.1193/070913EQS198M>
- American Association of State Highway and Transportation Officials. (2023). *AASHTO Guide Specifications for LRFD Seismic Bridge Design* (3rd Edition, 321 pp).
- American Society of Civil Engineers. (2016). *Minimum design loads and associated criteria for buildings and other structures* (ASCE 7-16). American Society of Civil Engineers, 822 pp.
- American Society of Civil Engineers. (2017). *Seismic Evaluation and Retrofit of Existing Buildings* (ASCE 41-17). American Society of Civil Engineers, 567 pp. <https://doi.org/10.1061/9780784414859>
- American Society of Civil Engineers. (2022). *Minimum Design Loads and Associated Criteria for Buildings and Other Structures* (ASCE 7-22). American Society of Civil Engineers, 975 pp. <https://doi.org/10.1061/9780784415788>
- Boore, D. M., Stewart, J. P., Seyhan, E., & Atkinson, G. M. (2014). NGA-West2 Equations for Predicting PGA, PGV, and 5% Damped PSA for Shallow Crustal Earthquakes. *Earthquake Spectra*, 30(3), 1057–1085. <https://doi.org/10.1193/070113EQS184M>
- Building Seismic Safety Council (BSSC). (2020). *NEHRP Recommended Seismic Provisions for New Buildings and Other Structures, Volume 1: Part 1 Provisions, Part 2 Commentary (FEMA P-2082-1)*. Building Seismic Safety Council, 555 pp.
- Campbell, K. W., & Bozorgnia, Y. (2014). NGA-West2 Ground Motion Model for the Average Horizontal Components of PGA, PGV, and 5% Damped Linear Acceleration Response Spectra. *Earthquake Spectra*, 30(3), 1087–1115. <https://doi.org/10.1193/062913EQS175M>
- Chiou, B. S.-J., & Youngs, R. R. (2014). Update of the Chiou and Youngs NGA Model for the Average Horizontal Component of Peak Ground Motion and Response Spectra. *Earthquake Spectra*, 30(3), 1117–1153. <https://doi.org/10.1193/072813EQS219M>
- Idriss, I. M. (1993). *Procedures for Selecting Earthquake Ground Motions at Rock Sites*. National Institute of Standards and Technology (NIST) Report GCR 93-265, 37 pp.
- Kuehn, N. M., Bozorgnia, Y., Campbell, K. W., & Gregor, N. (2023). A regionalized partially nonergodic ground-motion model for subduction earthquakes using the NGA-Sub database. *Earthquake Spectra*, 39(3), 1625–1657. <https://doi.org/10.1177/87552930231180906>
- Liu, C., & Macedo, J. (2021). New conditional, scenario-based, and non-conditional cumulative absolute velocity models for subduction tectonic settings. *Earthquake Spectra*, 38(1), 615–647. <https://doi.org/10.1177/87552930211043897>

- Luco, N., Ellingwood, B. R., Hamburger, R. O., Hooper, J. D., Kimball, J. K., & Kircher, C. A. (2007). Risk-Targeted versus Current Seismic Design Maps for the Conterminous United States. *Proceedings of the Structural Engineers Association of California 76th Annual Convention*, 13 pp.
- Newmark, N. M., & Hall, W. J. (1982). *Earthquake spectra and design*. Earthquake Engineering Research Institute, 103 pp.
- Pacific Earthquake Engineering Research Center/Applied Technology Council (PEER/ATC72-1). (2010). *Modeling and Acceptance Criteria for Seismic Design and Analysis of Tall Buildings (72-1)*. Applied Technology Council, 242 pp.
- Parker, G. A., Stewart, J. P., Boore, D. M., Atkinson, G. M., & Hassani, B. (2022). NGA-subduction global ground motion models with regional adjustment factors. *Earthquake Spectra*, 38(1), 456–493. <https://doi.org/10.1177/87552930211034889>
- Petersen, M. D., Shumway, A. M., Powers, P. M., Mueller, C. S., Moschetti, M. P., Frankel, A. D., Rezaeian, S., McNamara, D. E., Luco, N., Boyd, O. S., Rukstales, K. S., Jaiswal, K. S., Thompson, E. M., Hoover, S. M., Clayton, B. S., Field, E. H., & Zeng, Y. (2020). The 2018 update of the US National Seismic Hazard Model: Overview of model and implications. *Earthquake Spectra*, 36(1), 5–41. <https://doi.org/10.1177/8755293019878199>
- Powers, P. M., & Altekruze, J. M. (2022). *Nshm-conus-v5: National Seismic Hazard Model for the conterminous U.S. U.S. Geological Survey software release*. <https://doi.org/10.5066/P9J1OVR6>
- Powers, P. M., Clayton, B. S., & Altekruze, J. M. (2022). *Nshmp-haz-v2: National Seismic Hazard Model Project hazard applications and web services. U.S. Geological Survey software release*. <https://doi.org/10.5066/P9STF5GK>
- Rezaeian, S., Al Atik, L., Kuehn, N. M., Abrahamson, N., Bozorgnia, Y., Mazzoni, S., Withers, K., & Campbell, K. (2021). Spectral damping scaling factors for horizontal components of ground motions from subduction earthquakes using NGA-Subduction data. *Earthquake Spectra*, 37(4), 2453–2492. <https://doi.org/10.1177/87552930211027903>
- Rezaeian, S., Bozorgnia, Y., Idriss, I. M., Abrahamson, N., Campbell, K., & Silva, W. (2014). Damping Scaling Factors for Elastic Response Spectra for Shallow Crustal Earthquakes in Active Tectonic Regions: “Average” Horizontal Component. *Earthquake Spectra*, 30(2), 939–963. <https://doi.org/10.1193/100512EQS298M>